JOURNAL OF BACTERIOLOGY, Oct. 1981, p. 153-162
0021-9193/81/100153-10$02.00/0

Vol. 148, No. 1

Identification of Deoxyribonucleic Acid Restriction Fragments of β-Converting Corynebacteriophages That Carry the Gene for Diphtheria Toxin

GREGORY A. BUCK AND NEAL B. GROMAN*

Department of Microbiology and Immunology, School of Medicine, University of Washington, Seattle, Washington 98195

Received 3 April 1981/Accepted 19 June 1981

Deoxyribonucleic acid fragments bearing the gene for diphtheria toxin have been identified in restriction enzyme digests of deoxyribonucleic acids from β-converting and γ-nonconverting corynebacteriophages. A combination of physical and genetic evidence has established that the *Bam*HI band C fragment of β phage deoxyribonucleic acid, which carries the specific phage attachment site (Buck and Groman, J. Bacteriol. **148**:131-142, 1981), also carries most, and probably all, of the gene for diphtheria toxin. A detailed restriction map of this *tox*-bearing *Bam*HI fragment has been developed, and the locations and orientation of the *tox* gene and the *att*P site within this fragment have been established.

There are a variety of theoretical and practical questions that could be investigated if a DNA fragment carrying the structural gene for diphtheria toxin (*tox*) were isolated. These include questions of toxin structure, regulation of toxin synthesis and action, mechanisms of toxin secretion and entry into target cells, and the natural history and diagnosis of diphtheria. In principle, this isolation is possible since, in effect, the gene for diphtheria toxin has been cloned by nature by virtue of its inclusion in the genome of β-converting corynebacteriophage (17). In an accompanying paper (2), physical maps of the genomes of β-converting and γ-nonconverting corynebacteriophages were constructed on the basis of restriction enzyme and heteroduplex analyses. In addition, fragments in restriction endonuclease digests of β phage DNA which carry the vegetative phage attachment site (*att*P) were identified. This is of particular significance since it has been shown by genetic analysis that the *tox* gene is closely linked to the *att*P region (12, 14). Therefore, when a DNA fragment that carries the *att*P sequence is identified in a particular restriction enzyme digest this also locates the *tox*-bearing fragment or one closely associated with it.

In this communication, restriction fragments bearing *tox* are presumptively identified in hybridization experiments using toxin-specific mRNA as a radioactively labeled probe. These results are confirmed by data which correlate specific alterations in restriction endonuclease cleavage patterns with recombination within the gene for diphtheria toxin. In addition, a fine restriction map of one restriction fragment that contains both *att*P and *tox* is constructed, and the amino and carboxy terminus coding regions of the *tox* gene are oriented relative to this map.

MATERIALS AND METHODS

Strains of bacteria and phage. *Corynebacterium diphtheriae* strains C7(−)$^{tox^-}$, C7(β)$^{tox^+}$, C7(γ)$^{tox^-}$, C7(β-*tsr*-3)$^{tox^+}$, C7(γ-*tsr*-1)$^{tox^-}$, and C7(γ-*tsr*-2)$^{tox^-}$ were taken from the stock culture collection of this laboratory. The isolation of β-*h* *tox*$^-$(CRM45) phage and its lysogen is described in an accompanying paper (2). Bacterial mutants, C7(−)$^{tox^-}$*hm*723 and C7(β)$^{tox^+}$*hm*723, which are insensitive to iron repression of toxin synthesis (11), were generously provided by T. Uchida. Selective host strains C7/β^{vir} and C7/$\beta^{vir}\beta^{hc}$ were provided by R. Holmes.

Phage markers. Under the appropriate conditions, all of the β phage strains, except β-*h* *tox*$^-$(CRM45), produce intact, biologically active 62,000-dalton diphteria toxin and are thus designated *tox*$^+$(CRM62). Under similar conditions, β-*h* *tox*$^-$(CRM45) synthesizes a 45,000-dalton peptide that includes the amino terminus of the intact protein and cross-reacts serologically with diphtheria toxin (19). None of the γ strains produces any material that cross-reacts with toxin, and these strains are thus designated *tox*$^-$(CRM$^-$). Phages carrying host range mutations, *h* or *h'*, plaque on selective indicator strains C7/β^{vir} or C7/β, respectively, and the phages carrying both of these markers plaque selectively on indicator strain C7/β^{vir}/β^{hc} (9). Wild-type γ phage and its mutant derivatives carry the *h'* host range marker naturally. Phages carrying *tsr* (temperature sensitive repressor) mutations are heat inducible from the prophage state (8) and presumably have mutant repressor proteins.

Media. The TYE media used for the growth and maintenance of bacterial and phage stocks was de-

scribed previously (12). Low-phosphate TYE broth was made by precipitating the excess phosphate from normal TYE broth. The TYE broth was supplemented to 0.01 M $MgCl_2$–0.1 M $(NH_4)OH$, gently stirred for 30 min at room temperature, and held at 4°C overnight. The broth was passed through a Whatman no. 50 filter (Whatman Ltd., Clifton, N.J.) to remove the precipitate, adjusted to pH 7.2, and autoclaved.

Methods. All of the various methods used for the growth and maintenance of bacterial and phage stocks and the isolation of bacterial and phage DNA were previously described (12). The techniques required for restriction enzyme analysis, agarose gel electrophoresis, nitrocellulose filter blotting of agarose gels, isolation of specific restriction fragments, in vitro labeling of DNA with ^{32}P-deoxyribonucleotides and hybridization of radioactively labeled DNA probes to nitrocellulose filter-bound DNA are described in an accompanying paper (22).

Phage crosses and *tox* tests. Phage stocks of *β-h tox*$^-$(CRM45) and the appropriate *γ-h' tsr* phage were produced by UV or heat induction. Bacterial strain C7(−)$^{tox^-}$, grown to log phase in TYE broth, was pelleted (5 min, 5,000 × *g*) and suspended gently to a concentration of ca. 4×10^8 cells per ml in a mixture of 3.5 ml of the *β-h tox*$^-$(CRM45) phage stock and 1.5 ml of the *γ-h'tsr* phage stock. The suspension was supplemented to 0.002 M $CaCl_2$, equilibrated to 37°C, and incubated without aeration for 15 min to promote phage adsorption. The culture was then shaken gently at 37°C for 3 to 5 h, the remaining bacteria and debris were pelleted by centrifugation (5 min, 5,000 × *g*), and the lysate was plated at 10-fold and 100-fold dilutions in overlays containing C7/β^{vir}/β^{hc} to select for *hh'* recombinants. These plates were incubated overnight at 35°C, and isolated recombinant plaques were picked with sterile applicator sticks to fresh overlays seeded with C7(−). These C7(−) master plates were incubated overnight at 35°C, and the *hh'* recombinant phages were tested for their CRM phenotype by the in vitro gel immunodiffusion test (13). These tests detected three *tox* phenotypes, CRM45, CRM62, and CRM$^-$, and used lysogens of *β-tox*$^+$(CRM62) and *β-tox*$^-$(CRM45) phages as controls. To provide an adequate substrate for lytic growth of these phages, a small inoculum of host cells was picked from fresh C7(−)-containing overlays to each individual test site immediately before applying the recombinant phages. These overlays were prepared in low-iron *tox* test medium as a precaution against iron repression of toxin synthesis in phage-converted C7(−) cells. Each recombinant phage plaque was picked to one of the test sites already inoculated with C7(−), and the test plates were incubated for 2 to 4 days at 30°C. These tests were repeated several times, and the CRM phenotype of most of the recombinants was clearly established.

All of the recombinant phages that were CRM$^-$ or CRM62, some that were CRM45, and the few that did not give clearly readable results in the initial *tox* tests were selected for further investigation. These phages were picked from the master plate to 1 ml of TYE broth, diluted 10-fold, 100-fold, and 1,000-fold, plated on fresh C7(−)-containing overlays, and incubated overnight at 35°C. Seven clearly isolated plaques from each recombinant were picked from these plates to new overlays, one containing C7(−) and the other containing C7/$\beta^{vir/hc}$, and incubated overnight at 35°C. One clonally derived isolate from each recombinant that plaqued well on C7/$\beta^{vir/hc}$ was picked from the C7(−)-seeded overlay to 0.5 ml of TYE broth, and a C7(−) lysogen was produced (12). These lysogens were tested in the in vitro *tox* test at 30°C to confirm the *tox* phenotypes of the resident prophages.

In vivo labeling and purification of bacterial RNA. Bacterial strains were grown overnight at 30°C on TYE agar to provide fresh cultures. Cells were suspended to a concentration of ca. 6×10^8 cells per ml in 5 ml of low-phosphate TYE broth supplemented to 0.018 mM $FeSO_4$. The cells were washed twice by centrifugation (10 min, 5,000 × *g*) and resuspended in fresh low-phosphate TYE broth with $FeSO_4$, and the final pellet was resuspended in 5 ml of the same medium. Two milliliters of the cell suspension was then pipetted into a sterile screw-cap tube containing 0.3 mCi of [^{32}P]phosphate (Amersham Corp., St. Louis, Mo.). This culture was incubated for 40 min at 38.5°C, brought to 0.02 M sodium azide, and iced for 5 min. The bacteria were pelleted (10 min, 5,000 × *g*) and resuspended in 2 ml of cold (0°C) TYE with 0.02 M sodium azide. The cells were repelleted as above and resuspended in 1 ml of 0.05 M sodium acetate–4% sodium dodecyl sulfate–0.05 μg of bentonite per ml–1 mg of nuclease-free yeast RNA per ml.

The suspension was brought to 100°C in a boiling water bath and held at this temperature for 90 s. An equal volume of $CHCl_3$-isoamyl alcohol (24:1) was added, and the solution was agitated vigorously on a Vortex Jr. mixer (Scientific Industries, Inc., Queen Village, N.Y.) for 90 s. Phenol (1 ml) saturated with an aqueous solution of 0.01 M Tris–EDTA (pH 7.5) was added, and the cultures were mixed briefly as above and then incubated with vigorous agitation for 30 min at 55°C. During this step in the procedure, the cells lysed and the solution cleared. The solution was subjected to centrifugation (10 min, 5,000 × *g*) to separate the phases, and the aqueous phase, containing free nucleic acids, was collected. This solution was reextracted with an equal volume of buffer-saturated phenol, and the nucleic acid was precipitated with ethanol as described previously (18). The precipitate was dried, suspended in 0.01 M $MgCl_2$–0.04 M Tris (pH 7.0)–30 μg of RNase-free DNase (Worthington Diagnostics, Freehold, N.J.) per ml, and incubated for 4 h at 37°C. The DNase was removed by extraction with an equal volume of $CHCl_3$–isoamyl alcohol 24:1), and the remaining RNA was again precipitated with ethanol. The precipitate was dried and suspended in 1 ml of sterile distilled water.

To measure the purity of the RNA solutions, the percentage of the radioactive disintegrations per minute carried on material that was hydrolyzed in strongly alkaline conditions was assayed. From each sample, 5 μl was directly dried on a filter, 5 μl was directly precipitated in cold 5% trichloroacetic acid and collected on a filter, and 5 μl was incubated in 0.3 N NaOH at 37°C for 2 h, neutralized with HCl, trichloroacetic acid precipitated, and filter collected. The filters were dried, and for each the number of disintegrations per minute was determined in a Beckman LS-

100C scintillation counter (Beckman Instruments, Inc., Anaheim, Calif.). In every sample, more than 80 to 90% of the total activity was trichloroacetic acid precipitable, and more than 97% of the trichloroacetic acid-precipitable fraction was hydrolyzed in strongly alkaline conditions. Thus, most of the activity represented labeled RNA with very little contamination by alkali-stable DNA.

Hybridization of labeled RNA to nitrocellulose-bound DNA. Nitrocellulose filters prepared as described elsewhere (2) were placed in polyethylene bags, and a prehybridization mixture consisting of 2× SSC (1× SSC is 0.15 M NaCl–0.015 M sodium citrate), 2× Denhart solution (1× Denhardt solution is 0.02% each of Ficoll 400, polyvinylpyrrolidone, and bovine serum albumin [6]), 200 μg of yeast RNA per ml, and 0.02 M Tris (pH 7.6) was added. The bags were sealed and incubated for 12 to 16 h at 68°C. The pre-hybridization solution was then replaced with a similar fresh solution to which 8×10^6 dpm of purified in vivo-labeled RNA was added. The bags were resealed and incubated at 68°C for 16 to 18 h. The filters were washed (six times for 30 min each) in 2× SSC at 68°C, placed in pre-equilibrated 0.01 M NaCl–0.0005 M disodium EDTA–0.002 M Tris (pH 8.0)–40 μg of RNase A (Sigma Chemical Co., St. Louis, Mo.) per ml, and incubated at 37°C for 30 min. The filters were washed again (three times for 30 min each) in 2× SSC at 68°C, allowed to dry at room temperature, mounted on cellulose acetate sheets, sandwiched between Lightning Plus intensification screens (Du Pont Co., Wilmington, Del.) with Kodak RP-X-Omat film, and exposed for 1 to 5 days at −70°C.

RESULTS

Hybridization of β DNA with *C. diphtheriae* mRNA. Most of the β phage genes are repressed in the prophage state. However, at least two are expressed, the phage repressor gene and the *tox* gene (17). DNA fragments bearing particular genes expressed by the prophage can be identified by hybridizing mRNA produced by a C7(β) lysogen to DNA restriction fragments of vegetative β-*tsr*-3 phage. Radioactively labeled whole cell mRNA was isolated from cultures of a number of lysogenic bacterial strains under conditions allowing toxin synthesis, repression of toxin synthesis by excess ferrous ion, and induction of a β prophage. As a negative control, mRNA was also isolated from a nonlysogenic bacterial strain. The isolated mRNA from each bacterial culture was hybridized to nitrocellulose filter blots of *Sal*I and *Bam*HI restriction enzyme digests of vegetative β-*tsr*-3 phage DNA, and the blots were visualized by autoradiography. The results (Fig. 1) showed that the same *Sal*I (band B) and *Bam*HI (band C) fragments previously identified as bearing *att*P (2) also hybridized with mRNA from the uninduced, toxin-synthesizing lysogen, C(β)$^{tox^+}$*hm*723. mRNA from the nonlysogenic control, C7(−)$^{tox^-}$ *hm*723, and from the iron-sensitive control, C7(β)$^{tox^+}$, grown under conditions of iron repression, did not hybridize with any phage fragments. Also, as anticipated, mRNA from the induced lysogen, C7(β-*tsr*-3)$^{tox^+}$*hm*723, hybridized with many or all of the β-*tsr*-3 fragments.

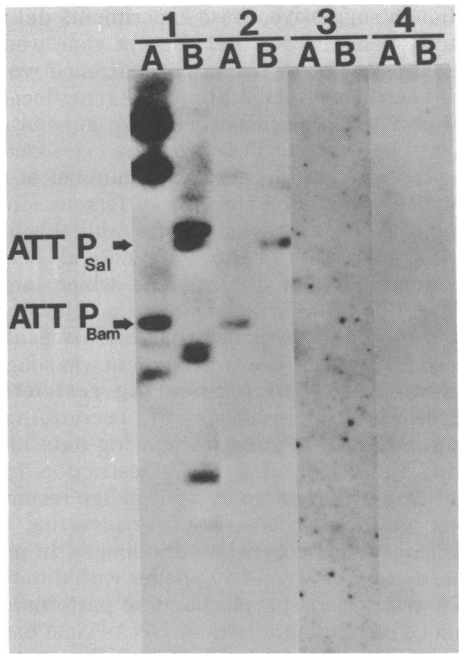

FIG. 1. *Hybridization of radioactive cellular RNA to nitrocellulose blots of restriction enzyme-cleaved vegetative phage DNA. Total cellular RNA was labeled in vivo with [^{32}P]phosphate, isolated, and hybridized to nitrocellulose filter-blotted agarose gels of restriction enzyme-digested phage DNA (see text). All strains from which RNA was extracted were grown under high-iron (0.018 mM $FeSO_4$) conditions which maximally repress transcription of the tox gene in toxinogenic C. diphtheriae (15). RNA was isolated from: 1, heat-induced C7(β-tsr-3)$^{tox^+}$hm723, which expressed both the vegetative phage functions and tox; 2, noninduced C7(β)$^{tox^+}$hm723, which expressed only prophage functions, i.e., repressor, and tox; 3, C7(β)$^{tox^+}$, which was sensitive to iron repression of tox and expressed only prophage functions; and 4, C7(−)$^{tox^-}$hm723, which provided a negative control. The labeled RNA was hybridized to nitrocellulose blots of restriction enzyme-cleaved DNA from vegetative β-tsr-3 phage: (A) BamHI digest, (B) SalI digest. The fragments of the BamHI ($ATTP_{Bam}$) and SalI ($ATTP_{Sal}$) restriction digests which were previously shown to carry the attP site of β phage DNA (2) are identified.*

The fact that the β-*tsr*-3 fragments which hybridized with mRNA from the toxin-expressing lysogen and the *att*P-bearing fragments (ATTP) were identical supported the conclusion that these were also the *tox*-bearing fragments.

Although suggestive, these experiments did not directly demonstrate that the *tox* gene was in these fragments. A similar concurrence would have been observed if other phage genes located near *att*P, e.g., the phage repressor gene or another unknown gene or genes, were expressed in the prophage state. There are a number of observations, including the role of ferrous ion in regulating the expression of *tox* and the high level of expression of the *tox* gene and, hence, the dominance of its mRNA, which argue against this alternative explanation. Nevertheless, more direct evidence that the *tox* gene is indeed on the *att*P-bearing fragment was sought.

Identification of *tox*-bearing restriction fragments by analysis of recombinant phage DNA. The most convincing data identifying the *tox*-bearing DNA restriction fragment came from an analysis of phage recombinants produced in crosses of β-converting and γ-nonconverting corynebacteriophages. In principle, a cross between two phages with different DNA restriction enzyme banding patterns can produce recombinants whose DNAs yield banding patterns different from those of the parental phages. A specific gene could be physically mapped to a particular restriction fragment if recombination within the gene or between closely linked markers flanking that gene were correlated with consistent changes in the restriction banding profiles. Such an analysis is facilitated if, as in the present case, the physical restriction endonuclease maps are known for the parent phages.

The genetic cross used in the present study (Fig. 2) was selected on the basis of the following information. Phages β and γ, which have slightly different restriction enzyme banding profiles (2, 4), also undergo genetic recombination (7). Two selective markers, *h* and *h'*, flank the *tox* gene in vegetative-phase DNA (10). The *hh'* segment of the genome covers only about 20% of the genetic map distance of β phage, but includes the *tox* gene, the *att*P site, and the region controlling phage immunity (10, 12). When *hh'* recombinants are selected in a cross between *tox*− strains of β and γ phages, nonselected *tox*$^+$ recombinants can be recovered at a detectable frequency (14). The selection of *hh'* recombinants limits the restriction fragments in which recombination occurs either to the *tox*-bearing fragment or to those fragments close to the *tox* gene. As seen from the figure, the toxin phenotypes of the *hh'* recombinant phages fall into three classes, i.e., CRM45, CRM62, and CRM$^-$, all of which can be identified by the agar gel

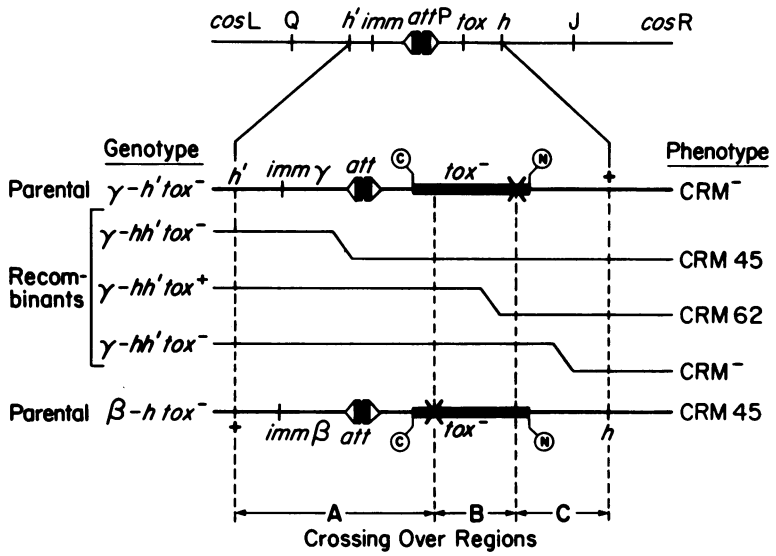

FIG. 2. *Vegetative crosses between β-tox⁻(CRM45) and γ-tox⁻(CRM⁻) corynebacteriophages. Vegetative crosses were carried out between β-h tox⁻(CRM45) and γ-h'tox⁻(CRM⁻) parental phages, and hh' recombinants were selected on indicator bacterial strain C7/β^{ts}/β^{hc}. Relative to the tox gene three phenotypic classes of phage, CRM45, CRM62, and CRM⁻, were produced by recombination in regions A, B, and C, respectively. The locations of the vegetative-phage attachment site (attP) and cohesive ends (cosL and cosR) are shown relative to the genes for phage immunity (immγ and immβ), diphtheria toxin (tox), host range (h and h'), and head and tail synthesis (Q and J, respectively). The orientation of the tox gene is shown relative to the other markers. The X's on the parental γ and β genomes denote the relative positions of the mutations that produce the CRM⁻ and CRM45 phenotypes in these phages, respectively.*

diffusion method (13). By comparing the DNA restriction profiles of *hh'* recombinants exhibiting the various CRM phenotypes to those of the parental γ and β strains, we have identified specific β and γ phage DNA restriction fragments that carry the *tox* gene.

Vegetative crosses were carried out between β-*h* *tox*$^-$(CRM45) and γ-*h'* *tox*$^-$(CRM$^-$). Two mutant strains of γ phage, γ-*tsr*-1 and γ-*tsr*-2 which differ slightly in their restriction digest banding patterns (4), were used in different crosses. The β strain carries a suppressible nonsense mutation in the *tox* gene (1) and produces a protein (45,00 daltons) which cross-reacts serologically with diphtheria toxin (19). The γ strains produce no cross-reacting material, but they carry at least a portion of the *tox* gene and recombine with β-*tox*$^-$(CRM45) strains to yield *tox*$^+$(CRM62) recombinants (14). The *hh'* recombinants were selected on indicator strain C7/β^{vir}/β^{hc}, and a number were tested for their *tox* phenotype. The results of three separate experiments are summarized in Table 1. Of the 943 *hh'* recombinants tested, approximately 97% had the CRM45 phenotype, 2.4% were CRM62, and 0.7% were CRM$^-$. In general, this indicates that the segment of DNA between the *h'* marker and the CRM45 mutation occupies most of the genetic map distance between *h'* and *h* and that the distances between the CRM45 and CRM$^-$ mutations and between the CRM$^-$ mutation and *h* are very small. The percentage of each phenotype provides only a rough approximation of these genetic distances since, as demonstrated below, there is an insertion (DI-2 loop) in the γ genome near the CRM$^-$ mutation. This inserted DNA is not homologous to β DNA (3) and probably decreases the frequency of recombination in this region.

Analysis of the vegetative cross between γ-h'*tsr*-2 *tox*$^-$(CRM$^-$) and β-h *tox*$^-$(CRM45). In the first experiment (Table 1, experiment 1), the *Bam*HI restriction digest banding patterns of DNA isolated from three CRM45, three CRM62, and two CRM$^-$ recombinants were compared with those of DNA from the parental strains (Fig. 3). Interestingly, restriction patterns from all of the CRM45 and CRM62 recombinants were identical to that of parental β phage. These results indicated that the parental β and γ phages have identical restriction banding patterns to the left of the *tox* gene, given the map orientation in Fig. 2. This conclusion was based on the fact that these two classes of *hh'* recombinants, which acquired the left arm of their genomes from γ parental phage, still had the restriction profile of β phage. The restriction

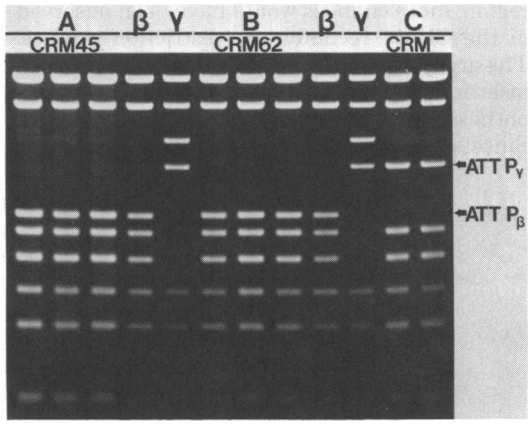

FIG. 3. *Restriction profiles of BamHI-digested recombinant phage DNAs, experiment no. 1: β-h tox*$^-$*(CRM45) × γ-h'tsr-2 tox*$^-$*(CRM*$^-$*). Phage DNA from selected recombinants was digested with BamHI restriction endonuclease and electrophoresed horizontally for 14 h through a 0.7% agarose gel at 50 V in TENA gel buffer. The lanes contain digests of DNA from: (A) three CRM45 recombinants, (B) three CRM62 recombinants, (C) two CRM*$^-$ *recombinants, (β) β-tsr-3 parental-type phage, (γ) γ-tsr-2 parental-type phage. The putative tox-bearing and attP-bearing β and γ fragments, ATTP*$_\beta$ *and ATTP*$_\gamma$*, respectively, are identified.*

TABLE 1. *tox* phenotypes of *hh'* recombinants isolated from vegetative crosses between β-*tox*$^-$(CRM45) and γ-*tox*$^-$(CRM$^-$) corynebacteriophages

Expt no.	Phages in cross	No. of recombinants (%) within crossover region[a] and resultant phenotype:			Total *hh'* recombinants (%)
		(A) CRM45	(B) CRM62	(C) CRM$^-$	
1	γ-*h'tsr*-2 *tox*$^-$(CRM$^-$) × β-*h tox*$^-$(CRM45)	295 (98.3)	3 (1.0)	2 (0.7)	300 (100)
2	γ-*h'tsr*-1 *tox*$^-$(CRM$^-$) × β-*h tox*$^-$(CRM45)	325 (94.7)	16 (4.7)	2 (0.6)	343 (100)
3	γ-*h'tsr*-1 *tox*$^-$(CRM$^-$) × β-*h tox*$^-$(CRM45)	293 (97.6)	4 (1.3)	3 (1.0)	300 (100)
	Totals	913 (96.9)	23 (2.4)	7 (0.7)	943 (100)

[a] See Fig. 2.

profiles of the CRM⁻ recombinants were also virtually identical to that of β phage, except that they contained a fragment associated uniquely with γ phage, whereas a smaller fragment found exclusively in the restriction profile of the β parent was absent. This particular change in restriction profile, i.e., the gain of a larger γ fragment (5.3 kilobases [kb]) and the loss of a single β fragment (3.9 kb), can only be explained by the presence of an extra sequence of DNA (ca. 1.4 kb), an insertion, in the region of the γ genome between the cross-over sites yielding CRM62 and those yielding CRM⁻ recombinants. If the restriction enzyme cleavage profiles of the parental phages differed in any other way in this region, more changes would have been observed in the CRM⁻ recombinant restriction profiles. The argument which leads to this conclusion, an insertion hypothesis versus a noninsertion hypothesis, is diagrammed and explained in Fig. 4. Since all of the CRM⁻ recombinants, but none of the CRM62 or CRM45 recombinants, exhibited this extra DNA sequence, it appears to be closely linked to the CRM⁻ mutation site and might, indeed, be responsible for that mutation. This additional piece of DNA is in all probability the 1.2 kb deletion-insertion loop (DI-2) observed in heteroduplexes of DNA from β and γ phages (2, 4). This conclusion was verified by heteroduplex analysis of the two isolated restriction fragments as reported in an accompanying paper (3).

The evidence given in this experiment alone clearly demonstrated that the β fragment which was lost and the γ fragment which appeared in the CRM⁻ recombinants contained a portion of the *tox* gene. In this phage cross the site of the CRM⁻ mutation was flanked by regions of the genome in which recombination on one side produced *hh'* CRM62 progeny, whereas recombination on the other side produced *hh'* CRM⁻ progeny. Since the switch from the CRM62 re-

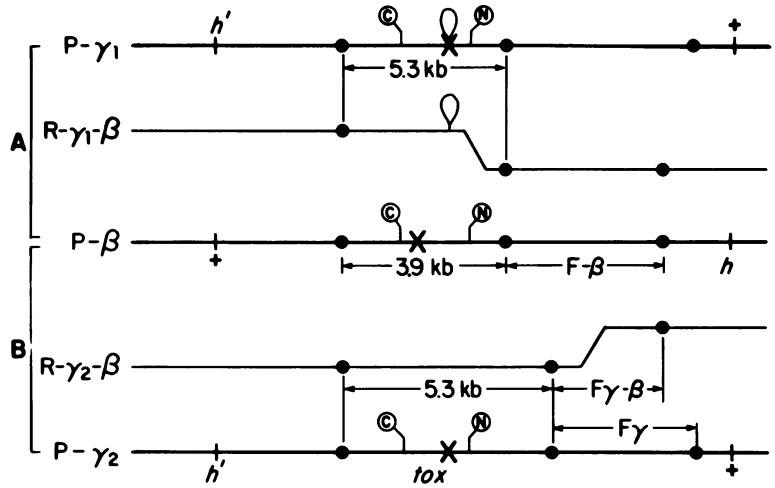

FIG. 4. *Two hypotheses examining the change observed in the DNA restriction profile of phage recombinants acquiring the CRM⁻ phenotype. This diagram of phage crosses illustrates two hypotheses for the origin of the CRM⁻ recombinant phages with unique restriction profiles (see Fig. 3 and text): (A) the insertion hypothesis and (B) the noninsertion hypothesis. P-β, P-γ1, and P-γ2 represent the parental β and γ phages in the two crosses, and R-γ1-β and R-γ2-β represent the respective CRM⁻ recombinant progeny. The solid circles (●) represent hypothetical restriction enzyme cleavage sites. In the fragments bearing the tox gene, its boundaries are defined by (N) and (C), the locations of the codons for the amino-terminal and carboxy-terminal amino acids, respectively. The X's identify the sites of the mutations in tox that produce the CRM45 and CRM⁻ phenotypes in parental β and γ phages, respectively. Fβ, Fγ, and Fγ-β are the hypothetical fragments that flank the right side of the tox-bearing fragments of P-β, P-γ2, and R-γ2-β, respectively. Host range (h and h') and tox markers are shown in the proper orientation. (A) The insertion hypothesis. In the cross between P-γ1 and P-β, it is assumed that the 5.3-kb tox-bearing fragment of P-γ1 differs from the 3.9-kb tox-bearing fragment of P-β by virtue of a 1.4-kb insertion of nonhomologous DNA within the tox gene. The restriction profile of the CRM⁻ recombinant, R-γ1-β, is identical to that of parental β phage, except that it contains the 5.3-kb γ fragment and lacks the 3.9-kb β fragment. (B) The noninsertion hypothesis. In the cross between P-γ2 and P-β, it is assumed that the parental DNAs are homologous, but that the difference in size of their tox-bearing fragments is due to a difference in the restriction enzyme cleavage sites. The CRM⁻ recombinant, R-γ2-β, also has a restriction profile which is similar to that of parental β phage, except that it contains a 5.3-kb γ fragment and lacks both the 3.9-kb β fragment and Fβ. It also contains a unique fragment Fγ-β, which is not present in either parental restriction profile.*

combinant to the CRM⁻ recombinant was correlated with the switch from the 3.9-kb β fragment to the 5.3-kb γ fragment, these fragments contain the site at which the CRM⁻ mutation occurred, i.e., a site within the *tox* gene or its regulatory sequences. In addition, it was shown that the 3.9-kb β fragment ($ATTP_\beta$) and the 5.3-kb γ fragment ($ATTP_\gamma$) carry the *att*P sites for β and γ phages, respectively (2, 3). In vegetative phage DNA the *tox* gene is oriented such that its carboxy terminus is closer to the *att*P site than to its amino terminus (9). Therefore, the 3.9-kb β fragment, and probably the 5.3-kb γ fragment as well, must minimally carry that portion of the *tox* gene from the site of the CRM⁻ mutation to the carboxy-terminus coding end of the gene. Since it is also known that, relative to the CRM45 mutation site, the site of the CRM⁻ mutation is proximal to the amino-terminus coding region of *tox* or even perhaps within a regulatory region (14), it is probable that these two fragments carry the sequences for virtually all of the *tox* gene. The coding sequence required for the entire structural *tox* gene is approximately 1.8 to 2.1 kb. Thus, both of these fragments could readily accommodate the entire gene.

Finally, these conclusions agree with those from the toxin-specific mRNA hybridization experiment in identifying *Bam*HI band C ($ATTP_\beta$) as the *tox*-bearing fragment in β phage DNA.

Analysis of the vegetative cross between γ-*h'tsr*-1 *tox*⁻(CRM⁻) and β-*h tox*⁻(CRM45). In two experiments (Table 1, experiments 2 and 3) where γ-*tsr*-1 phage replaced the γ-*tsr*-2 phage employed in the first cross, the *Bam*HI restriction profiles of DNA from *hh'* recombinants in the CRM45, CRM62, and CRM⁻ phenotypic classes were compared with those of the parental phages (Fig. 5). As noted in an accompanying paper (3), γ-*tsr*-1 phage stocks produced by heat induction contain a fraction of phage that carry a specific segment of bacterial DNA inserted into the $attP_\gamma$ site. The consequences of this insertion is the appearance of two unique (HET) DNA fragments, HETA and HETB, in the *Bam*HI restriction profiles of such γ-*tsr*-1 DNA. Interestingly, all six CRM45 and 11 CRM62 recombinants examined in these experiments had identical patterns that resembled the pattern of the β phage parent, but also included two HET fragments. The smaller of the HET fragments migrated in parallel with, and was presumably identical to, HETB, the smaller of the two HET fragments seen in the γ-*tsr*-1 DNA digests. The second HET fragment in these CRM45 and CRM62 recombinants, HETA', was different from any fragment found in either parent and smaller than the HETA band found in

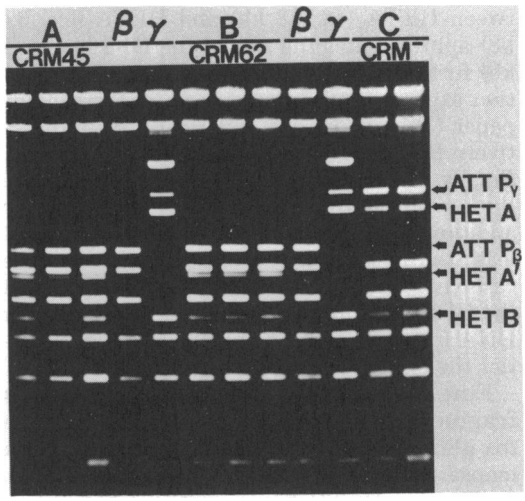

FIG. 5. *Restriction profiles of BamHI-digested recombinant phage DNAs, experiment no. 2: β-h tox⁻(CRM45) × γ-h'tsr-1 tox⁻(CRM⁻). Phage DNA from selected recombinants was digested with BamHI restriction endonuclease and electrophoresed horizontally for 14 h through a 0.7% agarose gel at 50 V in TENA gel buffer. The lanes contain digests of DNA from: (A) three CRM45 recombinants, (B) three CRM62 recombinants, (C) two CRM⁻ recombinants, (β) β-tsr-3 parental type phage, and (γ) γ-tsr-1 parental type phage. The putative tox-bearing and attP-bearing β and γ fragments, $ATTP_\beta$ and $ATTP_\gamma$, respectively, are identified. HETA and HETB, the HET restriction fragments in BamHI digests of parental γ-tsr-1 and CRM⁻ recombinant phage DNAs, and HETA', the HET fragment unique to digests of the CRM45 and CRM62 recombinant phage DNAs, are also identified.*

the γ-*tsr*-1 digests. In parallel with our previous finding, we assumed that the two HET fragments in digests of DNA from the CRM45 and CRM62 recombinants were products of *Bam*HI cleavage of bacterial DNA inserted in *att*P, presumably by the same mechanism proposed for this phenomenon in the γ-*tsr*-1 parent (3).

In contrast to the CRM45 and CRM62 recombinants, the five CRM⁻ recombinants examined gained the same 5.3-kb $ATTP_\gamma$ fragment described in Table 1, experiment 1, as carrying the *tox* gene and the DI-2 insertion and lost the corresponding 3.9-kb $ATTP_\beta$ fragment. Two HET fragments were also found in digests of these CRM⁻ recombinants, but these fragments migrated in parallel with HETA and HETB of the γ-*tsr*-1 parent. Since, as discussed above, only the CRM⁻ recombinants carried the DI-2 loop, it follows that HETA from the CRM⁻ recombinants and HETA' from the CRM45 and CRM62 recombinants are identical fragments, except that HETA carries and HETA' lacks the DI-2 loop. The fact that the size difference be-

tween HETA (ca. 4.8 kb) and HETA′ (ca. 3.4 kb) approximates the size of the DI-2 loop (1.2 kb) further supports this argument. Hybridization experiments reported in an accompanying paper (3), with HETA and HETA′ as radioactively labeled probes, verified this conclusion. Finally, since HETA′ carries the β site allelic to the γ site into which the DI-2 loop is inserted in addition to part of the *att*P site, it contains at least the portion of the *tox* gene between the carboxy-terminal coding region and the site of the CRM^- mutation. The size of this particular DNA fragment (ca. 3.4 kb) suggests that it carries the entire *tox* gene.

Fine mapping of the *Bam*HI restriction fragment of *β-tsr*-3 DNA that carries the *tox* gene. To construct more detailed restriction maps of the 3.9-kb *Bam*HI band C ($ATTP_\beta$), HETA and HETB were isolated, labeled with ^{32}P-deoxyribonucleotides by nick translation, and hybridized to nitrocellulose filter blots of *Hae*II and *Hinc*II restriction digests of the isolated $ATTP_\beta$ fragment (Fig. 6). HETA, which carries the *tox* gene and includes the adjacent part of *att*P (3), hybridized to fragments A and C in both the *Hae*II and *Hinc*II digests of $ATTP_\beta$. HETB, which carries the portion of $ATTP_\beta$ not carried by HETA including a part of *att*P (3), hybridized to bands B and A in the *Hinc*II digest and band B only in the *Hae*II digest. Thus, the *Hinc*II restriction products of the $ATTP_\beta$ fragment must be ordered B-A-C as depicted in Fig. 7. An analysis of *Hae*II partial digestion products of the $ATTP_\beta$ fragment showed that the *Hae*II restriction fragments were also ordered B-A-C.

These hybridizations also served to locate and orient the *tox* gene and the *att*P site on the $ATTP_\beta$ fragment (Fig. 7). Since both HET fragments hybridized to *Hinc*II fragment A, we concluded that *att*P is located within this fragment. In fact, because the HET fragments hybridized to nonoverlapping subsets of the *Hae*II restriction products of $ATTP_\beta$, the *att*P site is probably very near to the *Hae*II cleavage site separating *Hae*II fragments B and A. Therefore, the *tox* gene is within *Hae*II and *Hinc*II fragments A and C. It was oriented as shown because the carboxy terminus of the gene is proximal to the *att*P site. Finally, because the HETA fragment also carries the DI-2 loop,, the heteroduplex between the isolated 3.9-kb $ATTP_\beta$ fragment and the 5.3-kb $ATTP_\gamma$ fragment was oriented as depicted (Fig. 7). An electron micrograph of this heteroduplex was published in an accompanying paper (3).

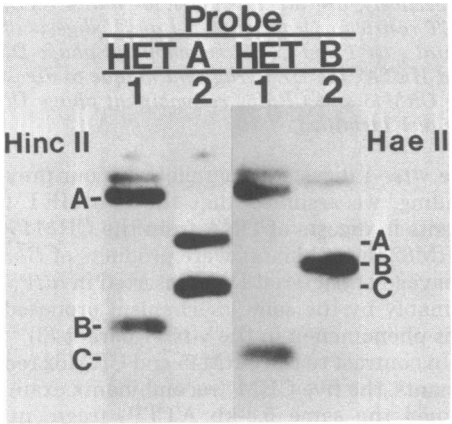

FIG. 6. *Fine structure mapping of $ATTP_\beta$ by hybridization with HETA and HETB. $ATTP_\beta$ was isolated from agarose gels, cleaved with HincII or HaeII restriction endonuclease, and electrophoresed for 1.5 h at 100 V into a vertical 1.2% agarose gel in TB buffer. The gels were blotted to nitrocellulose filter paper, and the blots were hybridized individually to in vitro-labeled HETA and HETB. 1, HincII restriction digest of $ATTP_\beta$; 2, HaeII restriction digest of $ATTP_\beta$. The relative positions of the final cleavage products of $ATTP_\beta$ with both HincII and HaeII endonucleases are shown. Less intense bands in these digests are partial restriction products that were used to confirm the order of the fragmments in the map.*

DISCUSSION

DNA fragments bearing the gene for diphtheria toxin have been identified in restriction enzyme digests of the genomes of β-converting and γ-nonconverting corynebacteriophages. Three lines of evidence converged to establish this finding. First, fragments carrying the vegetative-phase attachment site (*att*P) were identified in a number of restriction enzyme digests of β phage DNA (2). Since *att*P is closely linked to the *tox* gene, identification of the *att*P-bearing fragments was tantamount to the identification of the *tox*-bearing fragments or fragments near to them on the physical restriction maps of β phage DNA. Second, toxin-specific mRNA hybridized to the same restriction fragments that carry the *att*P site. Finally, and most persuasive, *Bam*HI band C ($ATTP_\beta$), the *att*P-bearing fragment in the *Bam*HI restriction enzyme digest of β phage DNA and the only fragment in this digest that hybridized to toxin-specific mRNA, was specifically identified as the *tox*-bearing fragment by analyzing changes in the restriction endonuclease patterns of selected recombinant phages. These hybrid phages were formed by recombination within the *tox* gene itself or within sequences closely linked to it. The fact that all of the restriction fragments identified as bearing *att*P or *tox* overlap on the various re-

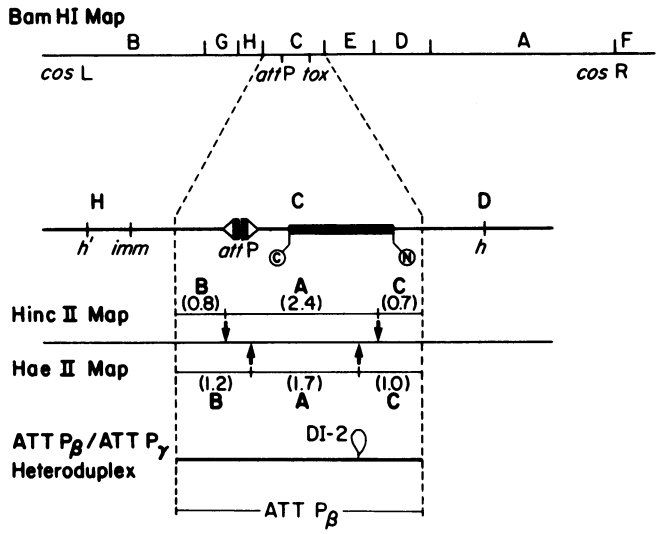

FIG. 7. *Fine-structure maps of ATTP$_\beta$. A fine restriction map of BamHI band C (ATTP$_\beta$) of β phage DNA was generated by using HincII and HaeII restriction endonucleases. The fine restriction map of ATTP$_\beta$ is shown oriented with the BamHI restriction map of the intact β-tsr-3 genome. The approximate size (in kilobases) of each of the HincII and HaeII fragments is given within parentheses. The relative positions of the attP$_\beta$ and tox are shown as is the orientation of the ATTP$_\beta$-ATTP$_\gamma$ heteroduplex containing the DI-2 loop. Genetic loci are as described in the legend to Fig. 2.*

striction endonuclease cleavage maps of β phage DNA reinforces these findings (2). Thus, all lines of evidence concur in identifying band C in the *Bam*HI restriction enzyme digests of β phage DNA (ATTP$_\beta$) as the *tox*-bearing fragment. By similar arguments band D in the *Bam*HI restriction enzyme digests of γ phage DNA (ATTP$_\gamma$) was also identified as bearing both the *att*P$_\gamma$ site and the *tox* gene.

The argument that all of the *tox* gene is present on ATTP$_\beta$ is the following. ATTP$_\beta$ is the smallest restriction endonuclease cleavage product known to carry both *att*P and *tox*. It carries ca. 3.9 kb of DNA and has a molecular weight of 2.6×10^6. The coding capacity required for diphtheria toxin, 60,000 to 70,000 daltons (16), is approximately 1.8 to 2.1 kb. Therefore, ATTP$_\beta$ carries roughly twice the capacity required for coding the structural gene for toxin. The ATTP$_\beta$-ATTP$_\gamma$ heteroduplex (3) (Fig. 7) provides additional information. The DI-2 loop divides this heteroduplex into a short arm with a 1.0-kb DNA sequence and a long arm with a 2.9-kb sequence. The *att*P site is on the long arm of this heteroduplex. Since all seven of the CRM$^-$ recombinants, but none of the 21 CRM62 recombinants, analyzed contain the DI-2 insertion, we assume that it is closely associated with, and probably the cause of, the CRM$^-$ mutation in the γ *tox* gene. In any event, these results require that the DI-2 loop be located closer to the amino terminus of the *tox* gene than to the site of the CRM45 mutation. Since the carboxy terminus of the *tox* gene is between *att*P and the CRM$^-$ mutation site (and the DI-2 loop) and *att*P is on the long arm of the ATTP$_\beta$-ATTP$_\gamma$ heteroduplex, the carboxy terminus of *tox* must also be on the long arm of this heteroduplex (Fig. 7). Therefore, under the most limiting assumptions, namely, that the DI-2 loop is immediately adjacent to the CRM45 mutation site, the ATTP$_\beta$ fragment carries the *tox* gene sequences for the region between the carboxy terminus and the site of the CRM45 mutation (15,000- to 20,000-dalton coding capacity) plus the coding capacity of the short arm of the ATTP$_\beta$-ATTP$_\gamma$ heteroduplex (30,000 to 35,000 daltons). Thus, at the very minimum, the ATTP$_\beta$ carries the coding capacity for 45,000 to 55,000 daltons of the toxin molecule. In addition, a mutant phage that produces a 20,000-dalton protein that cross-reacts serologically with diphtheria toxin has been isolated (9). Since CRM$^-$ strains do not produce any material that cross-reacts serologically with diptheria toxin, the CRM$^-$ mutation (the DI-2 loop) is probably closer to the amino-terminus region of *tox* than the CRM20 mutation. Finally, from our analysis of recombinants, it seems likely that the DI-2 loop is very close to or just precedes the amino-terminus coding region of *tox*. These observations lead to the conclusion that the entire intact structural gene of diphtheria toxin is carried on ATTP$_\beta$.

By similar logic, it can be concluded that

$ATTP_\gamma$ carries the entire structural toxin gene. However, the γ gene is inactive and carries the DI-2 insertion. In an accompanying publication (3), we have presented evidence that suggests that the DI-2 loop represents an insertion element or a transposon. This suggests that the *tox* gene of γ phage was inactivated by the insertion of the DI-2 sequences.

ACKNOWLEDGMENTS

A number of observations reported here are also reported by Costa et al. (5). We thank these authors for making a copy of their manuscript available before publication. We also acknowledge the technical assistance of Ruth Real in this study and thank Fred Heffron for helpful discussions and Kathy Spangler for help in preparing this manuscript.

This investigation was supported by Public Health Service Research grant A1-10492 from the National Institute of Allergy and Infectious Disease.

LITERATURE CITED

1. **Bacha, P., and J. Murphy.** 1978. Isolation and characterization of extragenic suppressor strains of *Corynebacterium diphtheriae*. J. Bacteriol. **136**:1135–1142.
2. **Buck, G. A., and N. B. Groman.** 1981. Physical mapping of β-converting and γ-nonconverting corynebacteriophage genomes. J. Bacteriol. **148**:131–142.
3. **Buck, G. A., and N. B. Groman.** 1981. Genetic elements novel for *Corynebacterium diphtheriae*: specialized transducing elements and transposons. J. Bacteriol. **148**:143–152.
4. **Buck, G. A., N. B. Groman, and S. Falkow.** 1978. Relationship between β converting and γ non-converting corynebacteriophage DNA. Nature (London) **271**: 683–685.
5. **Costa, J. J., J. L. Michel, R. Rappuoli, and J. R. Murphy.** 1981. Restriction map of corynebacteriophages β_c and β_{vin} and physical localization of the diphtheria *tox* operon. J. Bacteriol. **148**:124–130.
6. **Denhardt, D. T.** 1966. A membrane filter technique for the detection of complementary DNA. Biochem. Biophys. Res. Commun. **23**: 641–646.
7. **Groman, N. B., and M. Eaton.** 1955. Genetic factors in *Corynebacterium diphtheriae* conversion. J. Bacteriol. **70**:637–640.
8. **Groman, N. B., and W. Laird.** 1977. Heat-inducible mutants of corynebacteriophage. J. Virol. **23**:587–591.
9. **Holmes, R. K.** 1976. Characterization and genetic mapping of non-toxigenic (*tox*) mutants of corynebacteriophage beta. J. Virol. **19**: 195–207.
10. **Holmes, R. K., and W. L. Barksdale.** 1969. Genetic anlysis of tox^+ and tox^- bacteriophages of *Corynebacterium diphtheriae*. J. Virol. *3*:586–598.
11. **Kanei, C., T. Uchida, and M. Yoneda.** 1977. Isolation from *Corynebacterium diphtheriae* C7(β) of bacterial mutants that produce toxin in medium with excess iron. Infect. Immun. **18**:203–209.
12. **Laird, W., and N. B. Groman.** 1976. Prophage map of converting corynebacteriophage beta. J. Virol. **19**:208–219.
13. **Laird, W., and N. B. Groman.** 1976. Isolation and characterization of *tox* mutants of corynebacteriophage beta. J. Virol. **19**:220–227.
14. **Laird, W., and N. B. Groman.** 1976. Orientation of the *tox* gene in the prophage of corynebacteriophage beta. J. Virol. **19**:228–231.
15. **Murphy, J. R., J. L. Michel, and M. Teng.** 1978. Evidence that the regulation of diphtheria toxin production is directed at the level of transcription. J. Bacteriol. **135**:511–516.
16. **Pappenheimer, A. M., Jr.** 1977. Diphtheria toxin. Annu. Rev. Biochem. **46**:69–94.
17. **Singer, R. A.** 1976. Lysogeny and toxinogeny in *Corynebacterium diphtheriae*, p. 32–51. *In* A. W. Bernheimer (ed.), Mechanisms in bacterial toxinology. John Wiley & Sons, Inc. New York.
18. **Thomashow, M. F., R. Nutter, A. L. Montoya, M. P. Gordon, and E. W. Nester.** 1980. Integration and organization of Ti-plasmid sequences in crown gall tumors. Cell **19**:729–739.
19. **Uchida, T., A. M. Pappenheimer, Jr., and R. Greany.** 1973. Diphtheria toxin and related proteins. I. Isolation and properties of mutant proteins serologically related to diphtheria toxin. J. Biol. Chem. **248**:3838–3844.